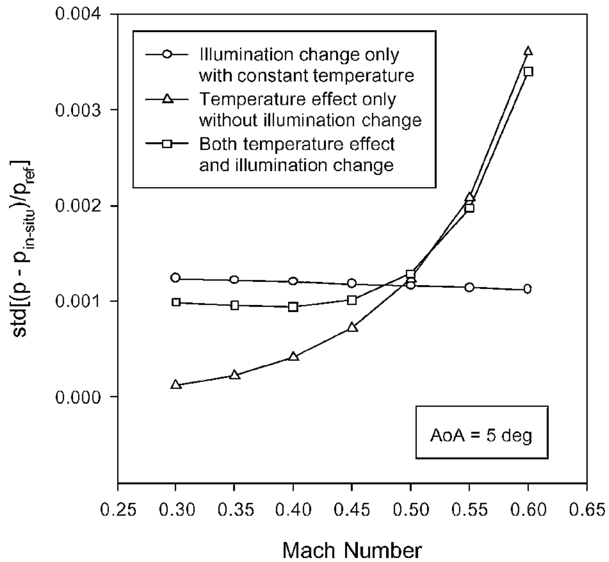

Fig. 5 Standard deviation of in situ PSP calibration error as a function of Mach number at AOA = 5 deg.

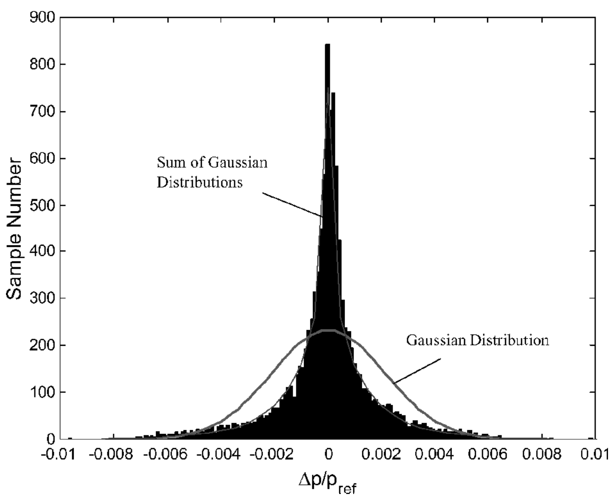

Fig. 6 Histogram of a union of all sample sets of in situ PSP calibration error over the whole range of AOA and Mach numbers.

Kammeyer et al.[5,6] found that the histogram of in situ calibration error was non-Gaussian for the overall set of samples over the whole range of AOA and Mach numbers. Figure 6 shows the simulated distribution for an overall set of samples of $\Delta p/p_{\text{ref}}$ (a total of 10,920 samples) over the whole range of AOA and Mach numbers, which duplicates the experimental non-Gaussian distribution given by Kammeyer et al. The Gaussian distribution with the same standard deviation is also plotted in Fig. 6 for comparison. In fact, for a union of sample sets having near-Gaussian distributions with different the standard deviation values at different AOA and Mach numbers, the distribution becomes non-Gaussian because more and more samples accumulate near zero when forming the union of the sample sets. The probability density function of a union of N sample sets is given by a sum of the Gaussian distributions rather than the Gaussian distribution, that is,

$$N^{-1}\sum_{i=1}^{N}\exp\left(\frac{-x^2}{2\sigma_i^2}\right)\bigg/\sqrt{2\pi}\,\sigma_i \tag{5}$$

As shown in Fig. 6, the distribution Eq. (5) correctly describes the simulated distribution. Note that we should not confuse this case with the central limit theorem that deals with a sum of independent random variables. Although the simulation is made for an airfoil section of a wing, the error for the wing can be estimated by averaging the local results over the full span of the wing. The behavior of the error for the wing should be similar to that for the airfoil.

Conclusions

In situ calibration uncertainty of PSP on the Joukowsky airfoil in subsonic flows is dominated by the temperature effect of PSP and the illumination change on surface due to model deformation, and therefore, it depends on AOA and Mach number. For a given AOA and Mach number, the probability density distribution of errors of in situ calibration conducted on the airfoil is near-Gaussian. However, the distribution becomes highly non-Gaussian for a union of all of the sample sets over the whole range of AOA and Mach numbers, which can be described as a sum of the Gaussian distributions. The simulation is consistent with the experimental results obtained by Kammeyer et al.[5,6]

References

[1] Liu, T., Campbell, B. T., Burns, S. P., and Sullivan, J. P., "Temperature- and Pressure-Sensitive Luminescent Paints in Aerodynamics," *Applied Mechanics Reviews*, Vol. 50, No. 4, 1997, pp. 227–246.

[2] Bell, J. H., Shairer, E. T., Hand, L. A., and Mehta, R. D., "Surface Pressure Measurements Using Luminescent Coatings," *Annual Review of Fluid Mechanics*, Vol. 33, March 2001, pp. 155–206.

[3] Sajben, M., "Uncertainty Estimates for Pressure Sensitive Paint Measurements," *AIAA Journal*, Vol. 31, No. 11, 1993, pp. 2105–2110.

[4] Liu, T., Guille, M., and Sullivan, J., "Accuracy of Pressure-Sensitive Paint," *AIAA Journal*, Vol. 39, No. 1, 2001, pp. 103–112.

[5] Kammeyer, M., Donovan, J., Kelble, C., Benne, M., Kihlken, T., and Felter, J. A., "Accuracy Assessment of a Pressure-Sensitive Paint Measurement System," AIAA Paper 2002-0530, Jan. 2002.

[6] Kammeyer, M., Kelble, C., Donovan, J., Benne, M., and Kihlken, T., "Recent Improvements in Pressure-Sensitive Paint Measurement Accuracy at Boeing," AIAA Paper 2002-2907, June 2002.

[7] Burner, A. W., and Liu, T., "Videogrammetric Model Deformation Measurement Technique," *Journal of Aircraft*, Vol. 38, No. 4, 2001, pp. 745–754.

R. P. Lucht
Associate Editor

Region of Flutter and Buckling Instability for a Cracked Beam

Q. Wang*
University of Central Florida, Orlando, Florida 32816-2450
and
C. G. Koh†
National University of Singapore, Singapore 119260, Republic of Singapore

I. Introduction

ANALYSIS of flutter and buckling of beams has long attracted attention in the applied mechanics community. The mathematical solutions for the critical force of a beam with different boundary conditions subjected to a nonfollower compression were given in the monograph by Timoshenko and Gere.[1] In addition, flutter analysis of a cantilever beam was also briefly conducted in the monograph. Beam buckling is an instability phenomenon referring to change of equilibrium state from one configuration to another one at a critical compression value. On the other hand, flutter is another type of beam instability when the vibration amplitude

Received 3 April 2003; revision received 7 July 2003; accepted for publication 15 July 2003.

*Associate Professor, Mechanical, Materials and Aerospace Engineering Department, 4000 Central Florida Boulevard; qzwang@mail.ucf.edu.

†Associate Professor, Department of Civil Engineering.

caused by initial disturbance grows without limit. This is usually because of the presence of a follower force applied to the beam structures.

It was Beck[2] who first solved the flutter instability of beam problem in view of dynamic analysis. Since then, the flutter of beams received considerable interests. The influence of an elastic support on the vibration and stability of a nonconservatively loaded was studied by Sundararajan.[3] In his paper the transition value of the translational spring at the free end of a cantilever beam was derived, and the coexistence of flutter and buckling in a system was first observed. Wang and Quek[4] investigated the potential of the piezoelectric materials in the enhancement of the flutter and buckling capacity of the beam just studied. The shift of the transition value of the spring stiffness was found when applying piezoelectric layer for the buckling and flutter control of the structure.

Cracks occurring in structural elements, such as beams and plates, affect the dynamic characteristics of structures. The understanding of the effect by the cracks is essential in the design of structures. For example, the study of the crack effects on the reductions of frequencies has led to the identification and detection of cracks.[5] The models of cracked beams have been proposed and applied to various engineering problems by many researchers. Dimarogonas[6] developed a general method to identify all of the possible direct and coupling spring effects for a prismatic beam with a surface crack. Papadopoulos and other researchers have investigated the coupling effect on structures caused by the presence of cracks.[7] They modeled cracks with local flexibility method and derived the flexibility matrix based on linear elastic fracture mechanics.

This Note concerns the region of flutter and buckling for a cracked-beam structure subjected to a follower force. The beam is fixed at one end and elastically supported at the other end. The results from the cracked beam studied herein are compared with those for the "healthy" (uncracked) beam studied before.[3,4] The coexisted instability phenomenon of the cracked-beam structure caused by elastic support is interesting in the field of structural stability and dynamics, as the understanding of the instability nature of a cracked structure will be helpful for its stability design. Therefore, the results are useful for the design and control of structures with potential cracks.

II. Region of Flutter and Buckling in the Cracked Beam

A cracked beam structure under a follower force P at its right end is shown in Fig. 1a. This beam is fixed at the left end and supported at the right end by a translational spring with stiffness value k. The beam of thickness h and length L is isotropic with Young's modulus E. A vertical crack, with depth h_1, is located at a distance L_1 from the left end of the beam. Let x denote the coordinate along the beam length with its origin at the left end and u the beam deflection defined to be positive downward.

The presence of a crack can be represented by a discontinuity in the slope at the location of the crack.[8] The total change of the slope of the beam at $x = L_1$ and the continuity of the deflection, rotation, and the shear, at the crack location are modeled as

$$\left.\frac{du_2}{dx}\right|_{x=L_1} - \left.\frac{du_1}{dx}\right|_{x=L_1} = \Theta \left.\frac{d^2u_1}{dx^2}\right|_{x=L_1} \tag{1}$$

$$u_1(L_1) = u_2(L_1) \tag{2a}$$

$$\left.\frac{d^2u_1(x)}{dx^2}\right|_{x=L_1} = \left.\frac{d^2u_2(x)}{dx^2}\right|_{x=L_1} \tag{2b}$$

$$\left.\frac{d^3u_1(x)}{dx^3}\right|_{x=L_1} = \left.\frac{d^3u_2(x)}{dx^3}\right|_{x=L_1} \tag{2c}$$

where $u_1(x)$ and $u_2(x)$ represent the deflection field of the beam for the domains of $0 < x < L_1$ and $L_1 \le x < L$, respectively. The parameter Θ represents the additional flexibility of the beam caused by the crack shown here:

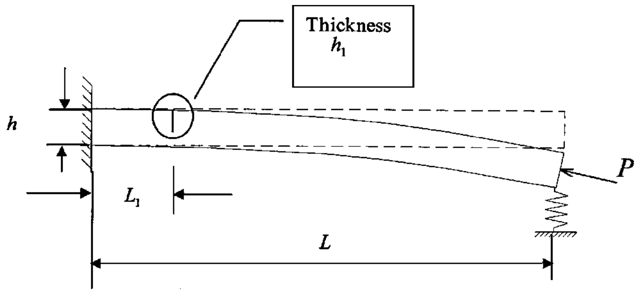

Fig. 1a Cracked beam fixed at one end and elastically supported at the other end.

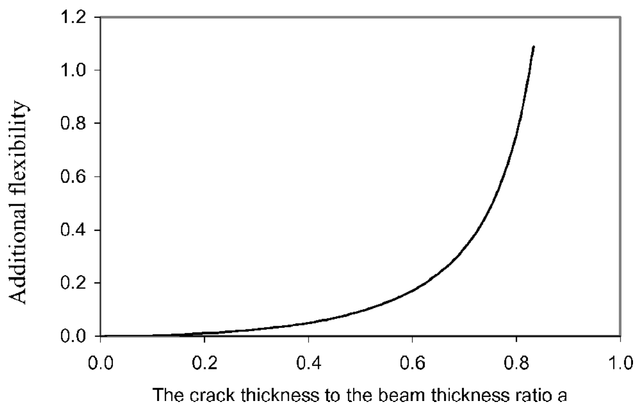

Fig. 1b Relation of the crack thickness and the additional flexibility parameter.

$$\Theta = 6\pi H \int_0^{\bar{a}} \left[\bar{a} F_{15}^2(\bar{a})\right] d\bar{a} \tag{3}$$

where $a = h_1/h$ and $F_{15}(a)$ is a correction function for stress intensity factor corresponding to a beam structure, given by

$$F_{15}^2(a) = \frac{\sqrt{\tan(\pi a/2)/(\pi a/2)}\{0.923 + 0.199[1 - \sin(\pi a/2)]^4\}}{\cos(\pi a/2)}$$

The region of the flutter and buckling of the cracked beam will be studied by finding the critical value of spring stiffness k above which the buckling capacity of the beam can exist. The beam under the follower force P is governed by the following equation:

$$EI\frac{d^4u(x)}{dx^4} + P\frac{d^2u(x)}{dx^2} = 0 \tag{4}$$

for which the general solution can be expressed as

$$u_1(x) = A_1 \cos\lambda x + A_2 \sin\lambda x + A_3 x/L + A_4, \qquad 0 < x < L_1 \tag{5}$$

$$u_2(x) = B_1 \cos\lambda x + B_2 \sin\lambda x + B_3 x/L + B_4, \qquad L_1 \le x < L \tag{6}$$

The boundary conditions of the cracked beam are shown here:

$$u_1(0) = 0 \tag{7a}$$

$$\left.\frac{du_1(x)}{dx}\right|_{x=0} = 0 \tag{7b}$$

$$\left.\frac{d^2u_2(x)}{dx^2}\right|_{x=L} = 0 \tag{8a}$$

$$EI\left.\frac{d^3u_2(x)}{dx^3}\right|_{x=L} = ku_2(L) \tag{8b}$$

Substituting the boundary conditions in Eqs. (7a) and (7b) into Eq. (5) yields

$$u_1(x) = A_1(\cos\lambda x - 1) + A_2(\sin\lambda x - \lambda x) \tag{9}$$

Similarly, $u_2(x)$ can be expressed in terms of B_1 and B_4 by substituting Eqs. (8a) and (8b) into Eq. (6) as follows:

$$u_2(x) = B_1\left(\cos\lambda x - \frac{\sin\lambda x}{\tan\lambda L} + \frac{EI\lambda^3 x}{kL\sin\lambda L}\right) + B_4\left(1 - \frac{x}{L}\right) \tag{10}$$

The region of the flutter and buckling of the cracked beam will be derived by solving an eigenvalue problem by substituting Eqs. (9) and (10) into the discontinuity of the rotation at the crack cite shown in Eq. (1) and the continuity conditions of the deflection, moment, and shear at the crack site, shown in Eqs. (2a–2c).

Finally the buckling equation for the cracked beam can be obtained as shown here involving the nondimensional parameter $\bar{k} = kL^3/EI$:

$$1 - \frac{\lambda L}{\tan\lambda L} + \frac{(\lambda L)^3}{\bar{k}\sin\lambda L} + \frac{\Theta}{L(\lambda L)^2}\left(\cos\lambda L_1 - \frac{\sin\lambda L_1}{\tan\lambda L}\right)\left(1 - \frac{L_1}{L}\right) = 0 \tag{11}$$

Let the critical value of $\bar{k}$ be $\bar{k}_c$; the regions of flutter and buckling of the beam can be classified as follows:

1) If $\bar{k} < \bar{k}_c$, flutter instability of the cracked beam is possible.

2) If $\bar{k} \geq \bar{k}_c$, buckling instability of the cracked beam is possible.

Under the following two cases, Eq. (11) can be reduced to the solution $1 - \lambda L/\tan\lambda L + (\lambda L)^3/\bar{k}\sin\lambda L = 0$ from which the transition value is $\bar{k}_{ch} = 34.85$ derived by Sundararajan[3]:

1) $\Theta = 0$, that is, there is no crack.

2) $L_1 = L$, that is, the crack is at the right end, and hence has no effect on the beam.

III. Numerical Results and Discussion

Next, numerical study is conducted pertaining to the region of the flutter and buckling of the cracked beam. Figure 1b presents the additional flexibility of the beam, Θ in Eq. (1), vs the ratio of the thickness of the surface-through crack to the beam thickness, $a = h_1/h$.

The transition value $\bar{k}_c$ vs the crack location at different values of $a = h_1/h$ is plotted in Fig. 2a. It is observed that $\bar{k}_c$ is small compared with that of the healthy beam, that is, $\bar{k}_{ch} = 34.85$, when the crack is located at $L_1/L < 0.45$. For example, the solution gives $\bar{k}_c \approx 26$ when $L_1/L = 0.05$ and $a = 0.45$. When the crack is located at $L_1/L \geq 0.45$, $\bar{k}_c$ is always bigger than the corresponding value of the healthy one, that is, $\bar{k}_{ch} = 34.85$. However, this value converges to $\bar{k}_{ch}$ at $L_1/L = 1$. Another investigation is that the higher the intensity of the crack is, the bigger difference is found for the transition value of the spring stiffness from $\bar{k}_{ch}$.

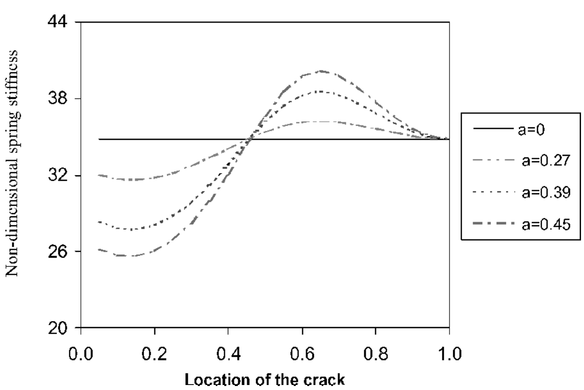

Fig. 2a Critical stiffness of the spring vs the location of the crack *L1/L*.

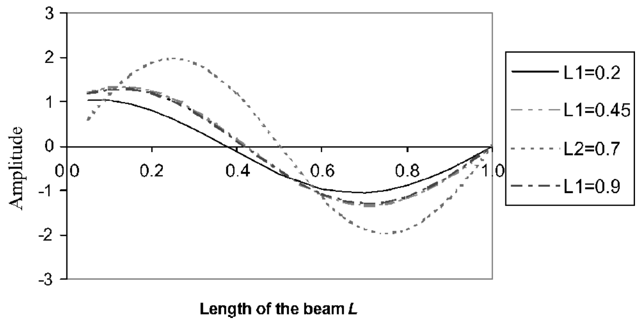

Fig. 2b Mode shape for curvature of the buckling beam.

Two critical locations of the crack, $L_1/L \approx 0.45$ and $L_1/L = 1$, are found from the preceding study based on Fig. 2a. At these two locations the transition value $\bar{k}_c$ is almost equal to $\bar{k}_{ch}$. This observation can be explained from Fig. 2b, which depicts the mode shape for the curvature of the cracked beam. It is found that when crack is located at $L_1/L \approx 0.45$ or $L_1/L = 1$ the curvature of the buckling beam is zero at the crack location and, according to Eq. (1), the discontinuity in rotation at the crack location vanishes.

IV. Conclusions

The Note studies the region of the two distinct instability forms, namely, flutter and buckling, for cracked beams. The numerical results show that the transition value of the elastic spring at the right end of the beam in Fig. 1a is smaller that the value for the healthy counterpart when the crack is located at $L_1/L < 0.45$, but the converse is true when $L_1/L \geq 0.45$. In addition, the transition value remains the same as that for the healthy beam when the crack is located at two specific locations, that is, $L_1/L \approx 0.45$ and $L_1/L = 1$. Further research will be focused on the stability analysis of the cracked structures by higher-order models of beam and /or finite element methods to increase the accuracy of the results. In addition, experimental results are expected to compare different crack models in deriving the results in the Note as well.

References

[1]Timoshenko, S. P., and Gere, J. M., *Theory of Elastic Stability*, McGraw–Hill, New York, 1961.

[2]Beck, M., "Die Knicklast des Einseitig Eingespannten Tangential Gedrukten Stabes," *Z. Angew. Math. Phys.*, Vol. 3, 1952.

[3]Sundararajan, C., "Influence of an Elastic End Support on the Vibration and Stability of Beck's Column," *International Journal of Mechanical Sciences*, Vol. 18, 1976, pp. 239–241.

[4]Wang, Q., and Quek, S. T., "Enhancing Flutter and Buckling Capacity of Column by Piezoelectric Layers," *International Journal of Solids and Structures*, Vol. 39, 2002, pp. 4167–4180.

[5]Cawley, P., and Adams, R. D., "A Vibration Technique for Non-Destructive Testing of Fibre Composite Structures," *Journal of Composite Materials*, Vol. 13, 1979, pp. 161–175.

[6]Dimarogonas, A. D., and Paipetis, S. A., *Rotor Dynamics*, Elsevier, London, 1983.

[7]Papadopoulos, C. A., "Torsional Vibrations of Rotors with Transverse Surface Cracks," *Computers and Structures*, Vol. 51, 1994, pp. 713–718.

[8]Krawczuk, M., and Ostachowicz, W. M., "Modeling and Vibration Analysis of a Cantilever Composite Beam with a Transverse Open Crack," *Journal of Sound and Vibration*, Vol. 183, 1995, pp. 69–89.

A. Chattopadhyay
Associate Editor